UNIVERSITY OF COPENHAGEN

Atmospheric photochemical loss of H and H2 from formaldehyde

the relevance of ultrafast processes

Simonsen, Jens Bæk; Rusteika, Nerijus; Johnson, Matthew Stanley; Sølling, Theis Ivan

Atmospheric photochemical loss of H and H₂ from formaldehyde: the relevance of ultrafast processes

Jens B. Simonsen,[b] Nerijus Rusteika,[a] Matthew S. Johnson[b] and Theis I. Sølling[ab]

We have performed *ab initio* calculations to examine the potential energy along the normal modes of ground-state HCHO and along the reaction coordinates for loss of H₂ and atomic hydrogen, respectively. This exploration showed that there are no specific features that will lead to reaction on the excited-state surfaces for excitations that are relevant to the troposphere and stratosphere. The calculations did however lead to the localization of a conical intersection point through which a specific loss of H₂ could take place. However, the conical intersection lies at 5.4 eV relative to the ground state molecule at equilibrium and is thus inaccessible *via* single photon excitation at tropospheric and stratospheric wavelengths. In addition to the *ab initio* investigation we have carried out a femtosecond pump–probe experiment using a 266/400 nm excitation. The results show that the timescale for the internal conversion from the initially prepared high-lying Rydberg states is on the order of a picosecond. This process populates the n → π* first excited singlet state which then survives for a substantially longer time before it is depopulated to form hot ground state or triplet-excited molecules that can then decompose.

Introduction

The topic of formaldehyde photochemistry is almost as old as the topic of photochemistry itself. Weisshar and Moore[1] have reviewed the early literature on the two decomposition channels of HCHO namely the loss of H₂ and atomic hydrogen on the S_1, T_1 and S_0 states. Already then it was apparent that the dynamical aspects of the processes are complex and difficult to address despite the limited size and high symmetry of the molecule. Matters did not become less complicated when a third pathway—the so-called roaming atom pathway—was experimentally and theoretically verified by Suits and Bowman.[2] A very recent thorough account of the problems pertaining to the dynamics of the formaldehyde decomposition has been given by Bowman and Zhang;[3] they conclude that the biggest remaining challenge lies in describing the dynamics related to the internal conversion and intersystem crossing processes between the involved states. Such issues are at the core of femtochemistry and are addressable in pump–probe studies with laser pulses of femtosecond duration.

One of the reasons for the widespread interest in the photolysis of formaldehyde is the important role it plays in the atmosphere. Formaldehyde is the most abundant carbonyl compound in the atmosphere and is a key intermediate in the photochemical oxidation of virtually all hydrocarbons. The principal removal occurs in the troposphere through photolysis and reaction with radicals such as OH.[4] The loss of H₂ and atomic hydrogen is accompanied by substantial ^{13}C and

[2]H isotope effects; the ^{13}C effect on the photolysis rate of HCHO has been found to be 0.894—a number that is significant when balancing the tropospheric carbon cycle.[5] In addition, it has been observed that the HCDO photolysis rate, j, is much smaller than that of HCHO in the troposphere, $j(\text{HCHO})/j(\text{HCDO}) = 1.58 \pm 0.03$, and that the branching ratio for molecular hydrogen formation from HCDO is much smaller than for HCHO; $j(\text{HCHO} \rightarrow \text{H}_2 + \text{CO})/j(\text{HCDO} \rightarrow \text{HD} + \text{CO}) = 1.82 \pm 0.07$. The difference in the rate of photolysis (j) in the radical channel is not as large, $j(\text{HCHO} \rightarrow \text{H} + \text{HCO})/(j(\text{HCDO} \rightarrow \text{H} + \text{DCO}) + j(\text{HCDO} \rightarrow \text{D} + \text{HCO})) = 1.10 \pm 0.06$.[6] In order to make a complete balance of the various isotopes in the tropospheric carbon cycle it is essential to fully understand the origin of the isotope effects.

Isotope effects are traditionally attributed to the changes that isotopic substitution brings about in the zeropoint vibrational energy and thus in the activation barrier of a chemical reaction. Alternatively, isotope effects can also be linked to classical and quantum dynamics.[7] The isotope effects seen in formaldehyde result from reactions that are initiated by light and thus excited-state surfaces are necessarily involved. In such cases the reactivity could be limited to involve a subset of the six degrees of freedom in formaldehyde. Such a reactivity pattern has previously been employed to account for the isotope effects on C–C cleavage in acetone.[8] In addition to the actual dissociation dynamics, the pre-dissociation dynamics are also central. This was previously illustrated in studies of excited-state ketones where internal conversion leads to activation of specific degrees of freedom. In the case of such pre-dissociation dynamics the key is the nuclear motions that are initiated when the ground-state geometry is placed on the Franck–Condon region of the excited state potential energy surface.[9] For photolytic formaldehyde

a Danish National Research Foundation Centre for Molecular Movies, University of Copenhagen, Universitetsparken 5, DK-2100 Copenhagen, Denmark
b Department of Chemistry, University of Copenhagen, Universitetsparken 5, DK-2100 Copenhagen, Denmark

decomposition, the dynamics of the internal conversion and intersystem crossing processes might also be central as these processes could possibly activate specific degrees of freedom as was found to be the case for excited-state ketones.[10,11] Through an experimental and theoretical investigation we address the non-adiabatic reactivity of formaldehyde, the focus is on the excited-state surfaces along a set of selected nuclear motions to address the coupling between modes through conical intersections and the possible specific activation of reactive modes.

Experimental

Experimental setup

The experimental setup consists of a commercial Ti:sapphire laser system from Spectra-Physics (Spitfire Pro) which delivers 100 femtosecond (fs) pulses, 1 mJ pulse^{-1} at 1 kHz. The regenerative amplifier is tuneable from 780–845 nm and was operated at 800 nm in the present work. This wavelength was then frequency doubled and tripled with two BBO crystals. The 266 nm pulse was passed onto an automated delay stage and merged with the 400 nm pulse before entering the sample chamber. The delay between the two pulses is controlled using a Labview routine. The two pulses intersect a molecular beam generated by expanding formaldehyde vapours seeded in He at 1.1 bar. The beam passes through a skimmer before entering the interaction region where the pressure is on the order of 10^{-6} mbar. The formaldehyde is released by heating para-formaldehyde mixed with $MgSO_4$ at 60 °C. The 266 nm pulse acts as a pump whereas the 400 nm pulse acts as an ionising probe. A time-of-flight mass spectrometer is used to record the temporal evolution of the ion current for ions formed in a pump–probe sequence.

Computational details

Calculations were carried out with the time dependent density functional theory (TD-DFT) and complete active space (CAS) formalisms in the GAUSSIAN98 suite of programs.[12] The ground-state geometry and vibrational frequencies were calculated at the B3LYP/6-31G(d) level of theory. This geometry was used as a starting point for all of the subsequent TD-DFT and CAS calculations.

At the TD-DFT level, the excitation spectra were calculated by employing the B3LYP functional and a small selection of basis sets to test the basis set performance for the subsequent potential energy surface scans. The basis set dependence is not striking. Basis set variation was also attempted in a CAS(6,8) calculation; in the case of the S_1 state (reached by an n $\rightarrow$ π* transition) we could only obtain reasonable agreement with experimental data for the double-zeta atomic natural orbital (ANO) basis of Roos and co-workers (Roos-dz).[13] This was then used for the remainder of the excited state CAS calculations. The starting guess on the orbitals was two oxygen lonepairs and one π-orbital for the occupied orbitals and three π*, one Rydberg 3s and a σ* orbital for the virtuals. These orbitals were obtained in a calculation of the ground-state geometry at the CAS(6,8)/Roos-dz level with a simple HF/STO-3G guess.

The equilibrium geometry at the first excited state was calculated at the CAS(6,8)/Roos-dz level with the ground-state geometry as a starting guess and the initial wave function from a CAS(6,8)/Roos-dz calculation of the vertical excitation. This procedure was also employed to calculate the geometry at the conical intersection between S_0 and S_1.

The excited-state potential energy surfaces in the direction of the displacement vectors associated with the ground-state normal modes were explored with TD-B3LYP/6-311+G(3df,2p); each mode was expanded in six steps on either side of the equilibrium geometry by successively adding 10% of the displacement vectors that result from the Gaussian output. For each of the geometries produced in this manner the seven lowest-lying excited states were calculated at the TD-B3LYP/6-311+G(3df,2p) level. The reaction coordinates for the H and H_2 losses were also explored. In the case of the H loss, the C–H bond was stretched from 0.9 to 1.9 Å in steps of 0.05 Å and at each frozen C–H bond length a partial geometry optimization was carried out at the B3LYP/6-31G(d) level of theory, for each of the resulting geometries the seven lowest vertical excitation energies were calculated at the TD-B3LYP/6-311+G(3df,2p) level. For the H_2 loss we employed the transition state located by Bowman and coworkers[14] and recalculated the CCSD(T)/aug-cc-pVTZ frequencies. To explore the PES along the imaginary mode it was treated as in the case of the ground-state vibrational frequencies except only to 0.3 of the displacement vector in each direction from the saddle point.

Results and discussion

It is the forces on the nuclei immediately after excitation, *i.e.* in the Franck–Condon region of the potential energy surface, that determine how the nuclei will move at very short time scales. For ultrafast and non-statistical bond breakage (<100 fs) to be in play, this motion must correspond to a bond stretch or, at least, include a component of a bond stretch. If that is not the case a slower and more statistical reactivity pattern will result where eventually all $3N - 6$ degrees of freedom are involved. The question is what determines the route from ultrafast to a totally statistical process and what lies in between. Are there any features of the ultrafast processes that can direct subsequent chemical processes, such as the passing of a conical intersection when going from one electronic surface to another? Such effects would strongly influence the size of isotope effects on a chemical reaction.

In the following, the ultrafast aspects of the loss of H_2 and atomic hydrogen from formaldehyde are explored. The most common route to insight concerning ultrafast processes is through femtosecond resolved pump–probe experiments. The spectral broadness of the fs pulse gives rise to the generation of a wavepacket. It is this intrinsic feature that opens the possibility of real-time observations of nuclear motions because wavepackets (as opposed to stationary states) can give rise to time-dependent observables. When the eigenstates are associated with *one* given nuclear motion, as for example $\nu = 0,1,\ldots,n$ of a given vibrational state, the observed signal is readily interpretable. The bandwidth of a 100 fs pulse is on the order of 250 cm^{-1}. Since the minimum number of vibrational

states in a superposition is necessarily two, it is really only very low-frequency vibrations that can give rise to a wavepacket which is spanned by $\nu = 0$ and $\nu = 1$ eigenstates when the excitation is brought about by a 100 fs pulse. Obviously, a wavepacket can be composed of individual vibrational eigenstates that are separated by a maximum of 250 cm^{-1} but the relation between nuclear motion and observables might be blurred. In such cases a theoretical investigation becomes indispensable for the unfolding of the experimental signal to nuclear motion.

Quite apart from the characteristics of the excited state surfaces with respect to bond breaking coordinates we have considered the relevance of the initial vibrational excitation on the ground state surface for the direction of energy to induce specific bond breakage. The hypothesis is that the vibrational excitation will be "carried over" to the excited state surface so that the initial motions immediately after the excitation will be influenced by the vibrations that took place on the ground state so that these are predetermining for the nuclear motions on the excited state surfaces.

The excited states of formaldehyde

The characteristics of the excited states in formaldehyde have been addressed in a wide variety of experimental and theoretical studies. The most recent theoretical studies clearly establish the nature of the excited states.[13,15] In the present study we have employed the TD-B3LYP/6-311 + G(3df,2p) method on geometries optimised at the B3LYP/6-31G(d) level whenever possible. The calculated excitation energies are shown in Table 1. Frisch *et al.* calculated the excited-state energies with the CIS-MP2 method and a series of basis sets. The values are included for comparison in Table 1. The best agreement with experiment was obtained when employing both diffuse- and polarization functions. The observed energetic ordering of the excited states is in agreement with that obtained experimentally and with our results if one disregards a missing Rydberg state in the work of Frisch (A_2, p-type).[16] Wiberg *et al.* have also reported the spectrum of formaldehyde calculated using TD-DFT with various functionals and a 6-311 + +G(d,p) basis set.[17] These values are also included in Table 1, our values lie within the range of those reported by Wiberg. In addition to a TD-DFT calculation of the excitation energies we have also performed a CAS-SCF calculation of the excita-

Table 1 Calculated excitation energies for the eight lowest singlet states

State	Excitation energies				
	This work^a	Ref. 15	Ref. 16	Ref. 17	Exp.^{b}
A_2 (n–π^*)	3.94	3.91–4.51	4.23–4.61	3.93–3.96	4.1
B_2 (n–3s)	6.83		8.62–18.18	6.58–6.98	7.13
B_2 (n–3p)	7.63		9.37–21.20	7.67–8.09	7.98
A_1 (n–3p)	7.84		9.54–14.49	7.35–7.93	8.14
A_2 (n–3p)	8.35			8.37–8.81	
B_1 (σ–π^*)	9.00		9.35–9.82	9.18–9.26	9.0
A_1 (π–π^*)	9.37		9.73–12.27		10.7
A_2 (π–π^*)	10.00				

^{a} B3LYP/6-311 + G(3df,2p) values in eV. ^{b} Values are taken from ref. 16.

tion energy to the lowest-lying singlet state. It was only possible to obtain reasonable agreement with experiment when the atomic natural orbital (ANO) basis set developed by Roos[13] was employed. In the case of an active space consisting of six electrons in eight orbitals, an excitation energy of 4.09 eV was obtained; this value was found to be quite independent of active space size. When Gaussian-type basis sets were employed, the excitation energies were calculated to be around 2.7 eV. Because the ANO basis set gives agreement between the calculated and the experimentally observed excitation energy it was used for further exploration of the S_1 state.

The ground-state vibrations on the excited state surfaces

At 0 K the nuclei of any given molecule move with a half-quanta of excitation in each vibrational mode. We have considered a scenario where the maximum overlap is between similar vibrational levels of the ground- and excited states. This means that the deactivation of the Franck–Condon species will take place through motions that are similar to those related to the ground state normal modes. Thus, we have explored the excited-state potential energy surfaces along the harmonic frequencies evaluated on the ground-state surface to investigate whether there is any strong interaction between the excited-state surfaces and the ground-state; an interaction could be manifested through closely-lying or crossing states. This could result in ultrafast internal conversion and possibly non-statistical activation of the involved degrees of freedom. The potential energy surface cuts are shown in Fig. 1. It is evident that in the case of the C=O stretch and the C–H asymmetric stretch there is a tendency for the higher-lying excited states to cross the lower-lying ones and in the case of C–H asymmetric stretch, the crossing with the ground state lies at the foot of an effectively repulsive (π–π^*) state.

Losing H and H_2, the ground-state reaction coordinate transferred to the excited-state surfaces

In relation to atmospheric photochemistry we have investigated the potential energy surfaces related to loss of a hydrogen atom and molecular hydrogen (Fig. 2 and 3). On the ground-state surfaces, the barriers are significant; in both cases on the order of 2 eV. The lowest lying electronic state is at 4 eV. A reaction on the ground state would necessarily involve an internal conversion from an excited state because an overtone excitation with a 2 eV (615 nm) photon to overcome the reaction barrier is a highly unlikely process. This motivates further exploration of the higher lying excited states to inspect whether the ground-state could be populated in a fast and specific manner to simulate non-statistical reaction dynamics and exceptional isotope effects. One additional question arises; namely whether the reactions could occur directly on the excited surfaces prior to randomisation of the available energy. To this end we have explored the excited states along the reaction path for H and H_2 loss on the ground state surface as a first order approximation to the reaction coordinate on the excited state surfaces. The potential energy surfaces along the C–H stretching coordinate are shown in Fig. 2. It can be seen
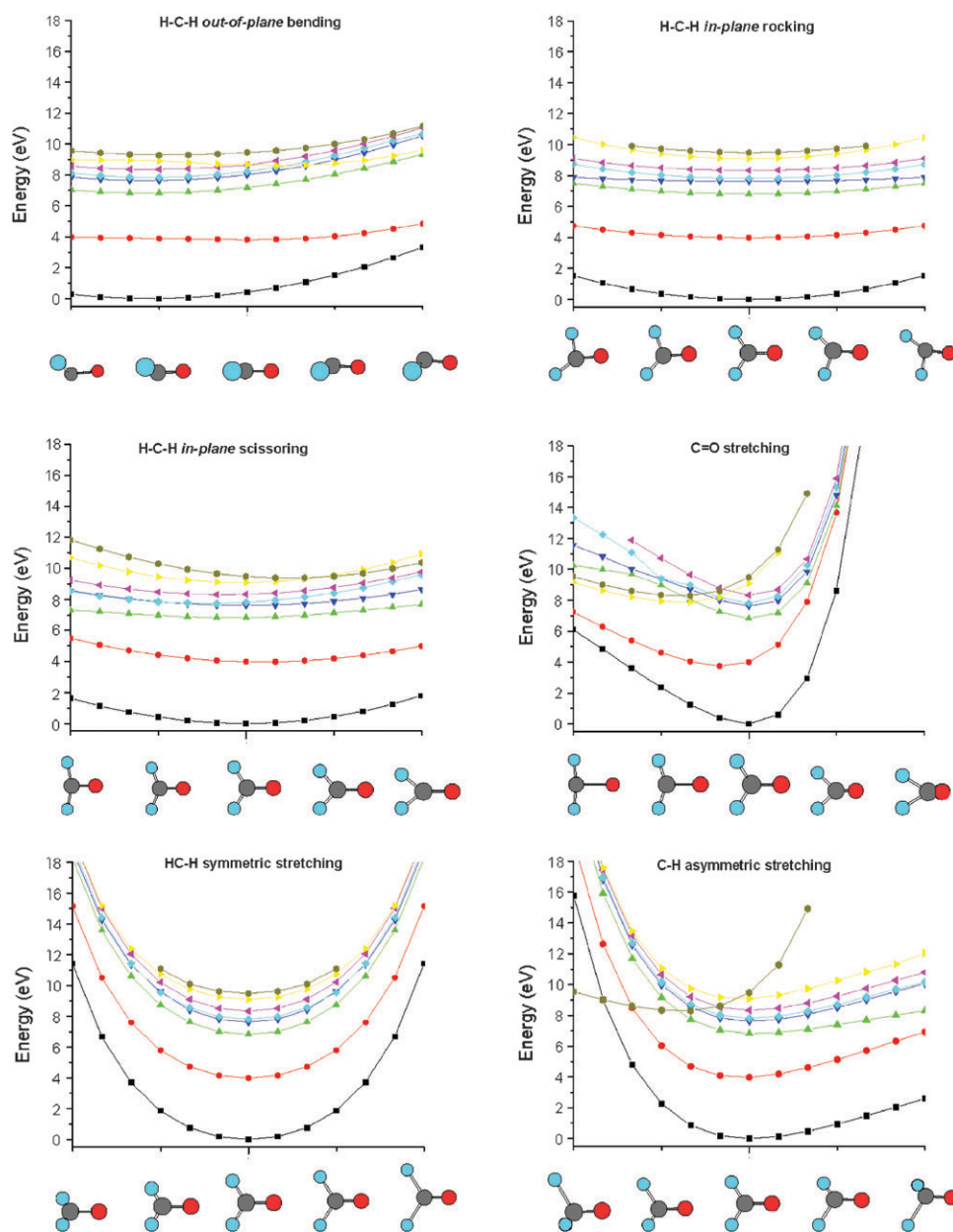
Fig. 1 Calculated potential energy surfaces of formaldehyde evaluated along the ground-state normal modes. The excitation energies are calculated at the TD-B3LYP/6-311 + G(3df,2p) level and the normal modes were calculated at the B3LYP/6-31G(d) level. The ordering of the states in the ground-state equilibrium region is the same as that in Table 1.

that there is no interaction between the excited-state surfaces and there is no indication of a preference for loss of a hydrogen atom from electronically excited HCHO. Thus, excitation of HCHO and subsequent activation of the C–H bond neither induces preferential excitation of the C–H bond, nor does it give rise to specific and non-statistical cleavage of the C–H bond, as the excited-state potential energy surfaces are parallel displacements of each other.

The situation is different for potential energy surfaces related to the loss of H_2 from formaldehyde (Fig. 3), in which case the surface along the ground-state minimum energy path down from the saddle point associated with H_2 loss differs significantly from several of those of the excited states. In fact, it would seem that there is no barrier for the association of H_2

and (excited) CO on S_1 (n–π*) whereas on S_2 (n–3s) the barrier persists although it is smaller than on the ground state. Yet again on S_3 (n–3p) the reaction proceeds without a barrier. What is noteworthy about this observation is that Rydberg potential energy surfaces generally have the same shape along a given coordinate.[18,19] The reason for this is that the ionic core of the Rydberg-excited species determines the shape of the potential energy surface (the Rydberg electron is too far away from the nuclei to influence the energy).[19] In this case the Rydberg states are the exception to the rule, one possible explanation could be that the Rydberg orbitals pointing in the direction of the C=O group are significantly polarized. This is shown in Fig. 4 where it can be seen that the 3p-orbital perpendicular to the molecular plane is clearly a
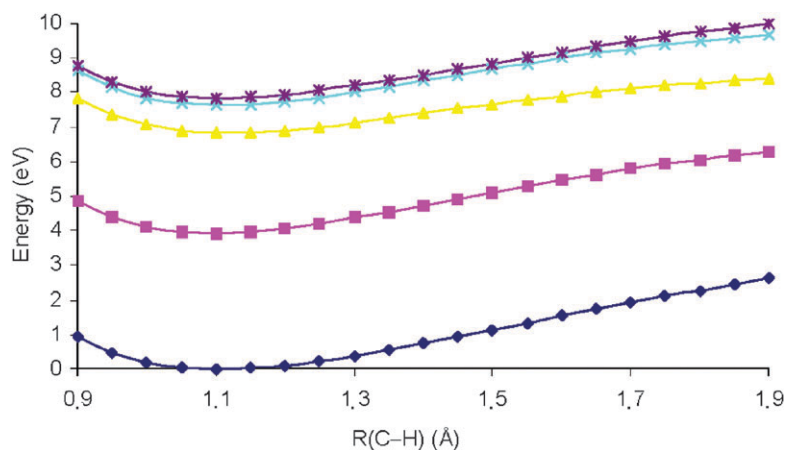
This journal is © the Owner Societies 2008

Phys. Chem. Chem. Phys., 2008, **10**, 674–680 | 677

Fig. 2 Calculated (TD-B3LYP/6-311 + G(3df,2p)//B3LYP/6-31G(d)) potential energy surfaces of formaldehyde evaluated along the C–H stretching coordinate. The ordering of the states in the ground-state equilibrium region is the same as that in Table 1.

genuine p-orbital whereas the one which points in the C=O direction is mostly situated on the oxygen atom. The same comment applies to the 3s orbital. We notice that the Rydberg surfaces in Fig. 1 and 2 are very similar and that the difference in the case of hydrogen loss might be a result of the complex nature of the reaction; a difference which shows that the assumption regarding the similarity of the Rydberg potential surfaces along a given coordinate does indeed have exceptions.

The barrier for H_2 loss is lower on S_3 compared to its ground state equivalent. However, there is no indication of a preferred mode of reaction on the excited states of formaldehyde. It is only in the case of a repulsive surface or direct activation of the reactive coordinate that a chemical process can compete with internal conversion between S_2 and S_3. We conclude that internal conversion or intersystem crossing precedes the loss of hydrogen and molecular hydrogen and that the excited state surfaces do not directly provide further insight into the isotope effects that are observed for the photoinduced tropospherical reactions of HCHO.

Direction of internal energy into reactive modes; conical intersections

As we have concluded that a photophysical process precedes the photo-induced decomposition of formaldehyde, it now remains to shed light on the nature of this process. To that end, we have explored S_0 and S_1 to locate a conical intersection that could give rise to fast and non-statistical population of the ground state, on which a (non-statistical) reaction could then take place. The search was guided by the potential energy surfaces evaluated along the normal modes.

An obvious candidate is the C=O stretching mode. This coordinate was argued previously to induce a non-statistical C–C bond breakage in acetone through the involvement of a conical intersection.[10,11] A guess-geometry taken at an extended C=O bond length along the C=O stretching coordinate (see Fig. 1). does indeed lead to a successful search for a conical intersection. However, the C=O bond has to be extended to 8 Å and the energy at the intersection is 10 eV at the crossing point between S_1 to S_0. Thus, this does not
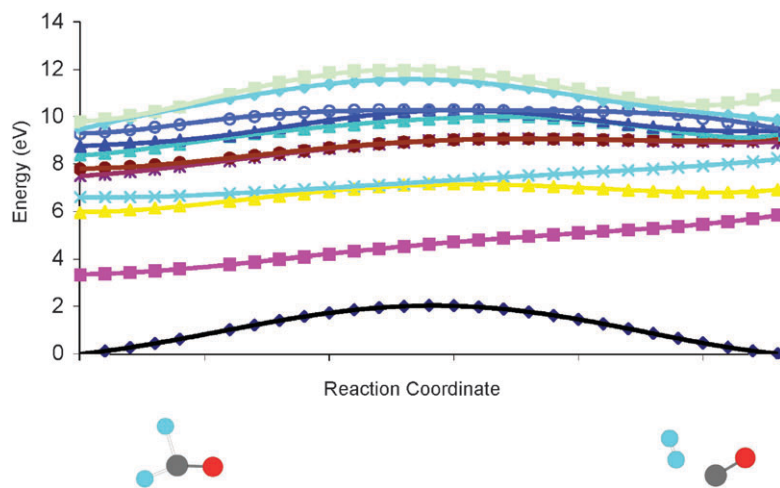

Fig. 3 Calculated potential energy surfaces of formaldehyde evaluated along the imaginary mode of the transition state for H_2 loss. The excitation energies are calculated at the TD-B3LYP/6-311 + G(3df,2p) level and the transition state structure and frequencies were calculated at the CCSD(T)/aug-cc-pVTZ level. The ordering of the states in the ground-state equilibrium region is the same as that of Table 1.
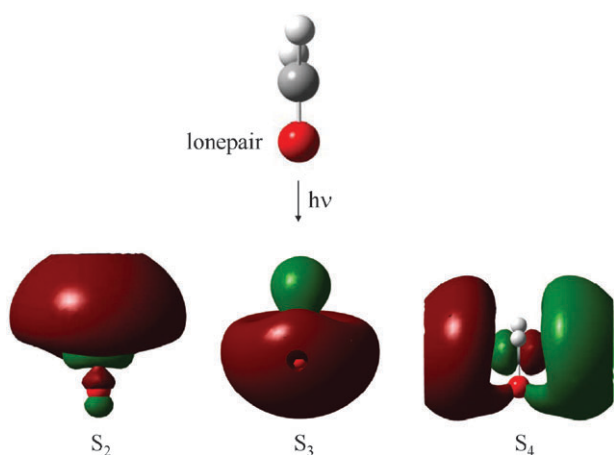
Fig. 4 The Rydberg orbitals involved in excitations to the lowest-lying singlet states. The shown orbitals are extracted from a TD-B3LYP/6-311 + G(3df,2p) calculation.

provide a viable pathway from S_1 to S_0. In addition to the C=O stretch there is a crossing along the C–H asymmetric stretch between S_1 and S_0. Further exploration of this coordinate does lead to the characterisation of a conical intersection. The structure at the intersection point is shown in Fig. 5 along with the gradient difference and derivative coupling vectors. A single-point calculation at the TD-B3LYP/6-311 + G(3df,2p) level shows that the energy at the intersection point is 5.4 eV relative to the equilibrium geometry at the ground state. This energy could be achieved by wavelengths shorter than 230 nm, for example a photon from the stratospheric UV window, 195–215 nm. An inspection of the gradient difference and the
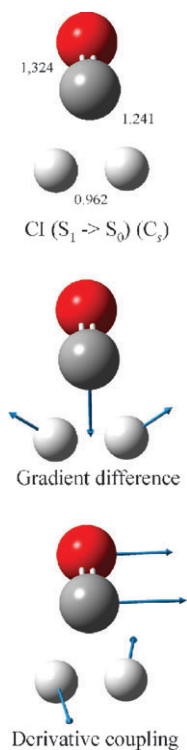

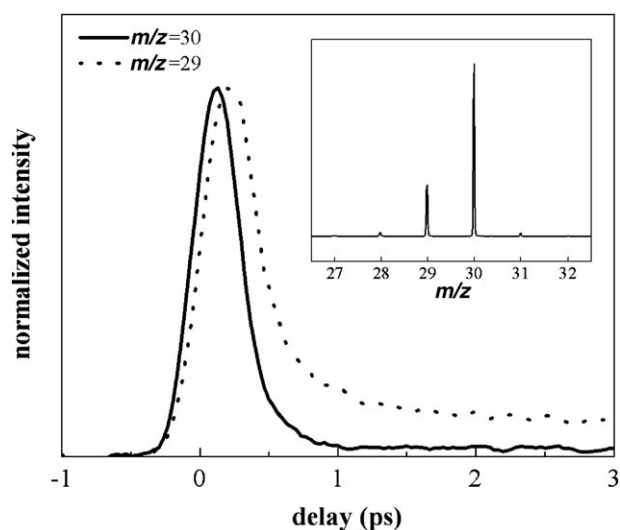**Fig. 5** Calculated geometry (CAS(6,8)/Roos-dz) at the conical intersection point.

Fig. 6 Temporal evolution of m/z 30 and m/z 29 from the mass spectrum shown in the top right. The data was obtained with 100 fs 266 nm pump pulses and 400 nm probe pulses.

derivative coupling vectors shows that the former points to the equilibrium region of S_1 whereas the latter is more consistent with the formation of CO and vibrationally excited H_2 (the product from the "roaming atom mechanism" proposed by Suits).[2] Photons with a wavelength shorter than 230 nm are not widely abundant in the atmosphere, and in any case the molecule is transparent in this region, thus it would seem unlikely for this conical intersection point to have relevance in relation to the large isotope effects that was found for H_2 loss.

Recently, substantial attention has been given to decomposition *via* the T_1 state.[20,21] This process was shown to specifically give rise to loss of a hydrogen atom. Thus, another reactive pathway could involve transition from S_1 to T_1 and thus not the ground-state altogether. Our search for conical intersections is aimed at revealing a direction of energy to specific degrees of freedom on the very short time-scale. The time-scales that we are aiming at are too short for the transition from S_1 to T_1 to be important with respect to activation of specific degrees of freedom. We have therefore not addressed the involvement of a triplet state. The actual decomposition, which takes place in nanoseconds or more, could in fact take place *via* a triplet state.

The femtosecond time-resolved mass spectra

The mass spectrum that results from excitation with a 266 nm photon and subsequent ($t = 0$) multiphoton ionization with 400 nm photons is shown in the inset of Fig. 6. The excitation with a 266 nm photon is used to mimic that taking place in the atmospheric UV window. The most abundant ions are those that correspond to ionised HCHO (m/z 30), ionised HCHO less a hydrogen atom (m/z 29) and ionised HCHO less H_2. The temporal evolution of the m/z 29 and m/z 30 ion currents (transients) is shown in Fig. 6. It can be seen that ionized HCHO (m/z 30) gives rise to a transient which is almost fully Gaussian shaped. This could be taken to indicate that the m/z 30 transient is purely a result of the increase in ionizing combinations when the pump and probe pulses are present

This journal is © the Owner Societies 2008

Phys. Chem. Chem. Phys., 2008, **10**, 674–680 | **679**

simultaneously (the so-called autocorrelation) and therefore solely reflects the folding of the temporal profiles of the pump and the probe pulses. In contrast to the findings for m/z 30 it can be seen that the m/z 29 transient is shifted by 125 fs relative to that of m/z 30. This indicates that a 125 fs process follows the pump excitation and precedes the formation of a neutral which upon ionisation gives m/z 29 (either by fragmentation of ionised HCHO or by direct ionisation of a fragment neutral). In addition to the shift, the m/z 29 transient also shows a picosecond component and a component that does not decay much further beyond 30 ps (not shown). The ion current of m/z 28 is too weak to obtain a decent transient, which shows that loss of H_2 from either the ion or the neutral is not a very favourable process.

The most obvious interpretation of the time-resolved data is that a two-photon excitation populates a highly excited Rydberg state which then subsequently (in 125 fs) equilibrates to form an S_n equilibrium species. In 2 ps the entire Rydberg population has internally converted to the S_1 state where the molecules stay until photophysical and/or photochemical processes depopulate S_1. The internal conversion process of HCHO and the persistent HCHO S_1 population is observed in m/z 29 and not in m/z 30 because the excited state HCHO molecules are vibrationally very hot, thus, after ionisation they will give rise to hot ions that will then decompose on their way out of the acceleration region of our instrument. The result that the excitation is a two photon process is in agreement with the computational finding that a one photon excitation would be symmetry forbidden with an oscillator strength of 0.

Conclusions

There is nothing in our calculations or experiments with 266 nm femtosecond pulses to indicate any ultrafast reactivity on the excited states of formaldehyde. The mechanism for photoinduced tropospheric loss of H and H_2 from formaldehyde would therefore seem to involve an internal conversion to a long-lived state, that is either the ground state or T_1, on which the reactions then take place on timescales that are dictated by statistics. From the time-resolved experiments we cannot fully rule out that loss of H and H_2 could take place on S_1 but it seems unlikely that it is a process of much general importance as the appearance energies for H and H_2 loss are on the order of 3.8 eV and the calculated S_1 barrier is on the order of 5.5 eV. The rather low appearance energies also show that the conical intersection point (5.4 eV) between S_0 and S_1 is not a direct player when it comes to explaining the isotope effects associated with the photochemical processes. Since a transition from S_1 to either T_1 or S_0 precedes the reaction and since a conical intersection is not involved in this process the explanation of the large isotope effects on atmospheric H_2-loss could be a result of the isotope induced differences in the coupling terms that are important in a vibronic coupling process of S_1 to either T_1 or S_0.

References

1 C. B. Moore and J. C. Weisshaar, *Annu. Rev. Phys. Chem.*, 1983, **34**, 525.
2 D. Townsend, S. A. Lahankar, S. K. Lee, S. D. Chambreau, A. G. Suits, X. Zhang, J. Rheinecker, L. B. Harding and J. M. Bowman, *Science*, 2004, **306**, 1158.
3 J. M. Bowman and X. B. Zhang, *Phys. Chem. Chem. Phys.*, 2006, **8**, 321.
4 K. L. Feilberg, M. S. Johnson and C. J. Nielsen, *J. Phys. Chem. A*, 2004, **108**, 7393.
5 K. L. Feilberg, B. D'Anna, M. S. Johnson and C. J. Nielsen, *J. Phys. Chem. A*, 2005, **109**, 2005–8314.
6 K. L. Feilberg, M. S. Johnson, A. Bacak, T. Röckmann and C. J. Nielsen, *J. Phys. Chem. A*, 2007, **111**, 9034.
7 M. S. Johnson, K. L. Feilberg, P. von Hessberg and O. J. Nielsen, *Chem. Soc. Rev.*, 2002, **31**, 313.
8 S. K. Kim, S. Pedersen and A. H. Zewail, *J. Chem. Phys.*, 1995, **103**, 477.
9 S. Nanbu and M. S. Johnson, *J. Phys. Chem. A*, 2004, **108**, 8905.
10 E. W. G. Diau, C. Kötting, T. I. Sølling and A. H. Zewail, *ChemPhysChem*, 2002, **3**, 57.
11 T. I. Sølling, E. W. G. Diau, C. Kötting, S. De Feyter and A. H. Zewail, *ChemPhysChem*, 2002, **3**, 79.
12 M. J. Frisch, G. W. Trucks, H. B. Schlegel, G. E. Scuseria, M. A. Robb, J. R. Cheeseman, V. G. Zakrzewski, J. A. Montgomery Jr, R. E. Stratmann, J. C. Burant, S. Dapprich, J. M. Millam, A. D. Daniels, K. N. Kudin, M. C. Strain, O. Farkas, J. Tomasi, V. Barone, M. Cossi, R. Cammi, B. Mennucci, C. Pomelli, C. Adamo, S. Clifford, J. Ochterski, G. A. Petersson, P. Y. Ayala, Q. Cui, K. Morokuma, D. K. Malick, A. D. Rabuck, K. Raghavachari, J. B. Foresman, J. Cioslowski, J. V. Ortiz, A. G. Baboul, B. B. Stefanov, G. Liu, A. Liashenko, P. Piskorz, I. Komaromi, R. Gomperts, R. L. Martin, D. J. Fox, T. Keith, C. Y. P. M. A. Al-Laham, A. Nanayakkara, C. Gonzalez, M. Challacombe, P. M. W. Gill, B. Johnson, W. Chen, M. W. Wong, J. L. Andres, M. Head-Gordon, E. S. Replogle and J. A. Pople, *GAUSSIAN 98, (Revision A.7)*, Gaussian, Inc., Pittsburgh, PA, 1998.
13 M. Merchan and B. Roos, *Theor. Chim. Acta*, 1995, **92**, 227.
14 X. B. Zhang, S. L. Zou, L. B. Harding and J. M. Bowman, *J. Phys. Chem. A*, 2004, **108**, 8980.
15 C. Angeli, S. Borini, L. Ferrighi and R. Cimiraglia, *J. Chem. Phys.*, 2005, **122**, 114304.
16 J. B. Foresman, M. Head-Gordon, J. A. Pople and M. J. Frisch, *J. Phys. Chem.*, 1992, **96**, 135.
17 K. B. Wiberg, R. E. Stratmann and M. J. Frisch, *Chem. Phys. Lett.*, 1998, **297**, 60.
18 J. L. Gosselin, M. P. Minitti, F. M. Rudakov, T. I. Sølling and P. M. Weber, *J. Phys. Chem. A*, 2006, **110**, 4251.
19 N. Kuthirumal and P. M. Weber, *Chem. Phys. Lett.*, 2003, **378**, 647.
20 W. Scott Hopkins, H.-P. Loock, B. Cronin, M. G. D. Nix, A. L. Devine, R. N. Dixon and M. N. R. Ashfold, *J. Chem. Phys.*, 2007, **127**, 064301.
21 H.-M. Yin, S. J. Rowling, A. Büll and S. H. Kable, *J. Chem. Phys.*, 2007, **127**, 064302.